Trees (2009) 23:79–84
DOI 10.1007/s00468-008-0256-1

ORIGINAL PAPER

A close-up view of wood structure and properties across a growth ring of Norway spruce (*Picea abies* [L] Karst.)

Michaela Eder · Karin Jungnikl · Ingo Burgert

Received: 30 August 2007 / Revised: 9 May 2008 / Accepted: 21 July 2008 / Published online: 6 August 2008

Abstract A growth ring of an adult Norway spruce (*Picea abies* [L] Karst.) was analyzed to a high resolution at the single cell level with respect to structural and mechanical changes during the growth period. For this purpose structural characterization was performed by means of light microscopy, scanning electron microscopy and wide angle X-ray diffraction for investigating the geometry of cells, their cell wall fractions and cellulose microfibril angles (MFA). The mechanical properties were determined in microtensile tests on individual tracheids which had been taken from sequentially cut tangential slices. The results revealed pronounced differences in tensile stiffness between earlywood and latewood cells but only minor differences in tensile stiffness between the cell walls of both tissue types. These comparatively small changes in cell wall stiffness across the growth ring were caused by slight changes in MFA. The findings suggest that trees mainly vary cell size to optimize water transport and mechanical stability during the growth period and that modification of the cell wall organisation plays a minor role.

Keywords Tree ring · Single cell · Gradual changes · Mechanical properties · Cell wall organisation

Communicated by T. Speck.

M. Eder (✉) · K. Jungnikl · I. Burgert
Department of Biomaterials, Max-Planck-Institute of Colloids and Interfaces, Wissenschaftspark Golm, Am Mühlenberg 1, 14476 Potsdam, Germany
e-mail: michaela.eder@mpikg.mpg.de

Introduction

Trees have to cope with competing optimization strategies during growth. On the one hand for efficient water transport, cells with large lumina and thin cell walls are needed, on the other hand mechanical stability demands higher cell wall proportions resulting in thick cell walls and small lumina. In conifers both functions are taken by one cell type, the tracheid, which serves for water transport in the earlywood and for mechanical stability in the latewood. This ongoing structural adaptation during growth makes the individual growth ring of a conifer a remarkable document of an iterative optimization process.

The adaptations of cell form and shape are seen even when observing a growth ring at low resolution, but cell size and cell wall thickness (density) might not be the only adaptable parameters. At the nanostructural level of the wood cell wall, trees manifest a wide variety of additional parameters such as the arrangement of cell wall layers, the chemical composition or the orientation of cellulose microfibrils. The microfibril angle (MFA) of the cellulose within the S2-layer of the wood cell wall is potentially the most powerful feature that can regulate the mechanical properties of a tracheid (e.g. Page and El-Hosseiny 1983; Reiterer et al. 1998; Yamamoto 1999; Yamamoto et al. 2001; Burgert et al. 2007). By adjusting the MFA the material properties of wood range from being stiff and strong (low MFA) to being flexible and tough (high MFA) (Reiterer et al. 1998).

Remarkable differences in nanostructural organisation and mechanical performance have been found in particular tissue types and have been related to their specific functionality, such as in compression wood, opposite wood or juvenile wood (Färber et al. 2001; Keckes et al. 2003; Burgert et al. 2007). However, the nanostructural adaptation

at the cell wall level across a normal adult wood growth ring has not yet been fully resolved.

Several investigations have been performed on the structure-property relationships of wood at and below the growth ring scale, aiming to better understand the structural and mechanical consequences of tree growth in normal wood. Jernkvist and Thuvander (2001) analyzed stiffness variation across a growth ring of Norway spruce by applying loads in the transverse direction and measuring strain fields in the radial-tangential-plane. They found that in the tangential direction, latewood is much stiffer than earlywood and that the stiffness of latewood in the radial direction (E_R) exceeded that of earlywood by a factor of 3. Elastic properties of individual early- and latewood layers were recently studied by e.g. Cramer et al. (2005) who performed measurements on small tissue samples of loblolly pine (air dried at 50% relative humidity). The longitudinal elastic moduli and the longitudinal-transverse shear moduli of earlywood and latewood tissues were discussed with respect to their position in the tree (growth ring and geographical location) and structural parameters (MFA and density). The authors reported that the ratios between the longitudinal elastic moduli of earlywood and latewood ranged from 0.6 to 7 with an average of 2.3. The ratio of the specific moduli (modulus normalized by specific gravity) was reported to be 1.2. In terms of the entire trunk, the modulus of elasticity increased with ring number and height.

Earlier work on thin earlywood and latewood tissue slices by Futó (1969), Ifju and Kennedy (1962) consistently showed increasing (longitudinal) moduli of elasticity and ultimate stresses from earlywood towards latewood, mainly as a consequence of increasing cell wall fraction and therefore density. Additionally, ultimate stress (calculated on the basis of cell wall cross-sectional area) was higher for latewood compared to earlywood. Similar trends for chemically isolated single cells have been shown by Schniewind (1966) and, recently by Mott et al. (2002). The observed differences between earlywood and latewood in ultimate stress, calculated on the basis of cell wall cross-sections (Mott et al. 2002), were explained by pitting and by variations in the MFA (the MFA in earlywood was 2.2% higher than in latewood).

In the present work we explored the gradual change of cell and cell wall parameters across one adult growth ring with high resolution. Mechanically isolated tracheids of consecutive slices were investigated in microtensile tests in wet conditions. We used an isolation technique where the cell wall polymers were not only retained in the most natural state but also the shape of the cells was preserved. Consequently there was no cell wall collapse as in pulped fibres. Hence, mechanical properties could be determined on the basis of both cell and cell wall cross-sections, allowing for the study of the adaptation across the growth ring at two hierarchical levels. Additionally, structural features were investigated by means of microscopy and wide angle X-ray diffraction (WAXD). The present data set could also serve as a basis for future work concerning the modelling of wood cell wall and tissue properties.

Materials and methods

A small block of adult wood ($\sim 2 \times 2 \times 2$ cm^3) of a $\sim$75 year old Norway spruce tree grown near Vienna containing the tree ring of interest was selected close to the cambium and near the base of the stem. Since the largest mechanical stresses occur in the periphery of the stem at its base "any structural adjustments made as a tree ages will be manifested most prominently in this region" (Niklas 1992; Jagels and Visscher 2006). Proper care was taken to exclude compression wood. The block was cut in the radial direction into two pieces. One block served for preparation of cross-sections, the other block was microtomed in the longitudinal-tangential direction (LT). Thirteen consecutive, 150 μm thin slices of the tree ring were produced and then served for the isolation of single tracheids. In order to retain the single cells in their natural state the isolation procedure was performed mechanically by using fine tweezers (Burgert et al. 2002, 2005a), dehydration was avoided by applying water. After isolation the cells were stored in glycerine to keep them in a wet condition. The remaining parts of the tissue slices were used for determining the MFA by wide angle X-ray diffraction (WAXD).

Microscopy

The cross-section of the wooden block, in particular the studied growth ring, was examined in the Low Vacuum mode of an environmental scanning electron microscope (ESEM, FEI Quanta 600) at low acceleration voltages.

Microtensile tests

The mechanical properties of the single cells were tested in tension by using a micromechanical testing device equipped with a 500 mN maximum capacity load cell. The glycerine-stored single cells were glued onto 200 μm thick foliar frames using cyanoacrylate glue (Burgert et al. 2004). The foliar frames carrying the individual cells were fixed by a pinhole assembly (Burgert et al. 2003) and were strained with a test speed of 1.5 μm/s. For strain measurements with sufficient accuracy, elongation was recorded by video-extensometry. During testing the samples were kept wet with humid air at room temperature. The stress calculation was based on cell and cell wall cross-sections. For this purpose the cross-sectional areas were determined in the ESEM at

the Low Vacuum mode. For further details see Burgert et al. (2005b). Between 7 and 15 successful measurements were performed for each tissue slice, resulting in 155 tracheids in total.

Microfibril angle measurements

Wide angle X-ray diffraction experiments on the LT-slices were carried out at a sample-detector distance of 5 cm using CuKα radiation (wavelength 1.54 Å) selected by a bent multilayer. A Nanostar (Bruker AXS) instrument was used and each pattern was collected with a 2D position sensitive (Hi-Star) detector for 1 h. The 2D patterns were corrected for background, radially averaged from scattering angle 2θ 21° to 24° and the intensity was plotted versus the azimuthal angle. The MFA was calculated according to the method described by Lichtenegger et al. (1998) using the 002 reflection. Considering the slice thickness of 150 µm and a beam cross-section of about 800 µm, each calculated value represents an average MFA of about 50 (earlywood) to 200 (latewood) tracheids.

Results

The scanning electron micrograph on the upper part of Fig. 1 and on the lower part of Fig. 5 show the cross-section of the analyzed adult growth ring of Norway spruce with a typical gradual transition from earlywood (left) to latewood (right). In the diagram (Fig. 1), black rectangles represent cross-sectional areas of the tested single cells taken from the individual slices whereas the white rectangles show the results obtained for the cell wall cross-sections. In terms of the cell cross-section a wave like trend was observed with rather high cross-section values up to slice 11 and with a local minimum in slice 5. Slices 12, 13

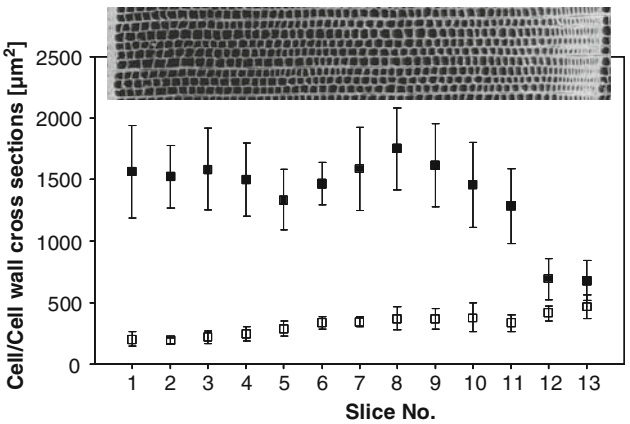

Fig. 1 Dimensions of cell (*black rectangles*) and cell wall (*white rectangles*) cross-sections across the growth ring. *Error bars* show standard deviation

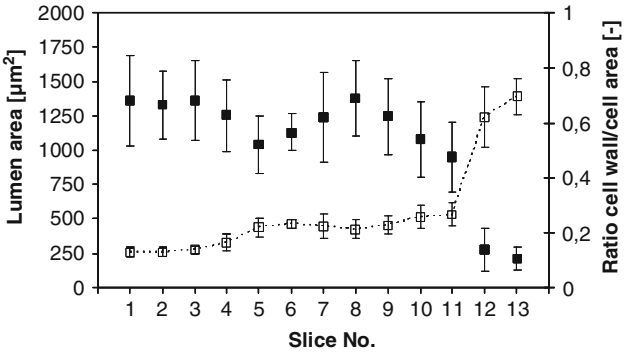

Fig. 2 Lumen area (*black rectangles*) and ratio cell wall/cell cross-sections (*white rectangles*) across the growth ring. *Error bars* show standard deviation

showed a significant reduction in cell cross-section. In contrast, the increase in cell wall cross-sectional area from earlywood towards latewood was almost gradual.

The cell and cell wall cross-section data were used to calculate two parameters describing microstructural changes across the growth ring (Fig. 2). (i) The lumen area (cell wall cross-section subtracted from the cell cross-section) as a relative measure of the conductivity of the structure (black rectangles). (ii) The second calculated parameter was the ratio of cell wall cross-section to cell cross-section which is related to tissue density (white rectangles). The latter increased by a factor of 5 across the tree ring (from 0.13 (slice 1) to 0.70 (slice 13)). The ratio results show an increase from slice 4 to 5 and followed by a plateau until slice 11 with a final pronounced increase in slices 12, 13. In contrast, the trend of the lumen area across the growth ring was similar to the cell cross-section (see Fig. 1) without a considerable decrease of lumen area until slice 11 and a local minimum for slice 5.

The crucial role for the structural variation for the tensile stiffness across the growth ring is shown in Fig. 3 by means of the averaged tensile moduli of the individual tracheids taken from the consecutive slices, both calculated on the basis of cell cross-section (black rectangles) and cell wall cross-section (white rectangles). The tensile stiffness calculated on the basis of the cell cross-sections was slightly increasing up to slice 4. A "step-like" increase took place from slice 4 to 5, followed by a rather constant tensile stiffness until slice 11. At the transition to the terminating latewood band (slice 11, 12) the stiffness of the entire cells increased dramatically. In contrast to the stiffness of the cells, the stiffness of the cell wall (white rectangles) remained rather constant along the whole tree ring (with the exception of the first slice). This indicates that a further adaptation at the nanostructural level is only minor. The averaged ultimate stress of the tested fibres is depicted in Fig. 4. Black rectangles show the ultimate stress calculated on the basis of cell cross-sections, white

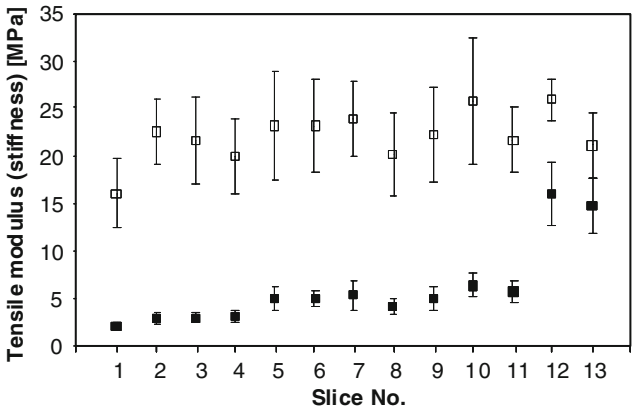

Fig. 3 Tensile modulus (stiffness) of the single cells, calculated on the basis of cell (*black rectangles*) and cell wall cross-sections (*white rectangles*). *Error bars* show standard deviation

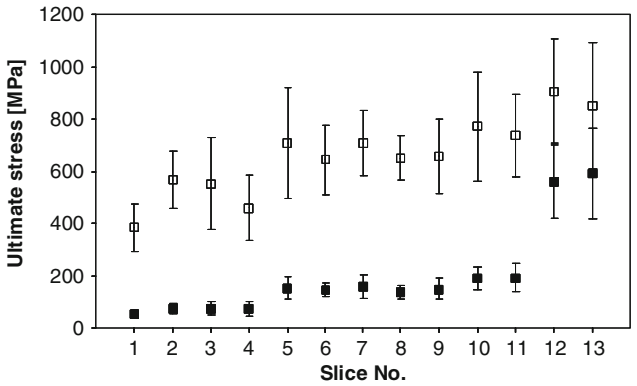

Fig. 4 Ultimate stress of the single cells, calculated on the basis of cell (*black rectangles*) and cell wall cross-sections (*white rectangles*). *Error bars* show standard deviation

rectangles show the results calculated on the cell wall cross-sections. In terms of the ultimate stress of the cells, the trend across the growth ring resembled the stiffness of the cells (see Fig. 3), and a strong correlation was found between ultimate stress and stiffness at the cell level ($R^2 = 0.92$). Again two abrupt rises were detected, from slice 4 to 5 and from slice 11 to 12 respectively.

In contrast, the ultimate stress of the cell wall diverged from the trend observed for the stiffness (correlation between ultimate stress and stiffness at the cell wall level: $R^2 = 0.38$). The ultimate stresses calculated on the basis of the cell walls increased in a stepwise manner comparable to the ultimate stresses of the cells but less pronounced.

In Fig. 5 the stiffness and the ultimate stress of the cell walls and the related MFA were plotted with respect to the specific position of the tracheids in the tree ring. Dots display the tensile stiffness of the cell walls, rectangles represent the measured MFAs and triangles display the measured ultimate stresses. Neighbouring data points within Fig. 5 showed that even very small changes in the MFA were immediately

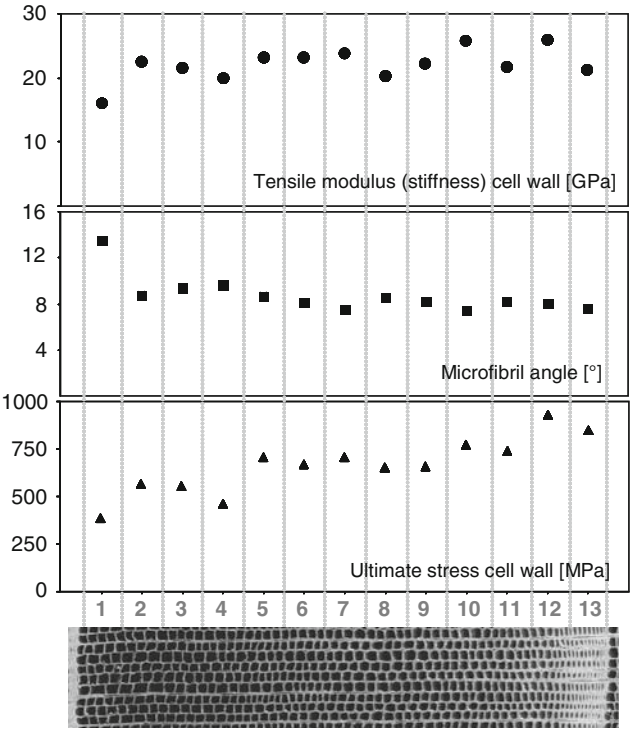

Fig. 5 Cell wall tensile modulus/stiffness (*circles*), microfibril angle (*rectangles*) and ultimate stress of the cell wall (*triangles*) across the growth ring

reflected in changes in tensile stiffness in the opposite direction (with the exception of slice 13). However, when plotting the MFA versus the tensile stiffness, no correlation of the data was found ($R^2 \sim 0.14$) which could be explained by the small changes in both mechanical (stiffness) and structural (MFA) properties. However, the ultimate stress of the cell walls did not follow the trend of the other parameter. The small variations in MFA were not reflected in the ultimate stress of the cell wall.

Discussion

In this paper, structural and mechanical parameters across a growth ring were studied with high resolution allowing for a detailed analysis of adaptational growth. Besides the pronounced changes in the transition from earlywood to latewood, smaller transitions (from slice 4 to 5), not obviously observed at the growth ring scale, were detected in all investigated parameters. However, due to the highly time consuming nature of these methods only one growth ring could be analyzed. Therefore the findings cannot be generalized but they indicate possible strategies of a tree to adjust cell and cell wall properties across growth rings.

By investigating the growth ring organisation at the level of the individual tracheid the interdependencies between the sub-micro and the meso-scale in the hierarchical structure

of wood were highly reflected. In the mechanically isolated tracheids the natural composition of the cell wall polymers was retained (Burgert et al. 2005a) allowing for a study of cell walls close to the native condition. Furthermore, the cells did not collapse during the isolation treatment as well known for chemically isolated tracheids (Page et al. 1977; Groom et al. 2002). Hence, in microtensile tests on mechanically isolated tracheids, properties related to both cell and cell wall could be determined.

The trends of the "density" (ratio of cell wall cross-section to cell cross-section) and cell lumen area (cell cross-section divided by cell wall cross-section) across the growth ring point to an interesting interrelation at the tissue level (Fig. 2). The interplay of both parameters sheds light on a possible strategy of the tree in optimizing both water transport and mechanical stability. By keeping the cell cross-section almost constant until reaching the severe latewood region (slices 12, 13) and increasing gradually the cell wall cross-section, the lumen size of the cells can be maximized in the general set up of an increasing density profile.

The comparison between cell and cell wall stiffness (Fig. 3) showed different trends of both parameters across the growth ring. The data indicates that the drastic increase in tensile stiffness in latewood is mainly due to changes in cell geometry (density, respectively) and that adaptations at the cell wall level are of less significance.

The ultimate stress of the cells increased from earlywood towards latewood, resulting in a factor of ~ 10 between the ultimate stress of earlywood and latewood tracheids (Fig. 4). This remarkable difference could be directly related to the increasing cell wall proportion (and therefore density) with increasing duration of the growth period. A drastic increase in ultimate stress occurred mainly at the cell level close to the latewood region (slices 12, 13).

At the cell wall level, the trend towards higher values across the growth ring was more pronounced for ultimate stress than for tensile stiffness. The ultimate stress of latewood, calculated on the basis of cell wall cross-sections, was almost twice as high as for earlywood. This phenomenon was already observed by Mott et al. (2002). Within the scope of their work they compared the mechanical properties of chemically isolated earlywood and latewood fibres. They showed that the ultimate stress of their latewood tracheids was 73% higher than that of earlywood fibres and related the large differences between early- and latewood to differences in the MFA (the calculated MFA was 2.2% higher in earlywood) and to pitting. Our data suggests that the increase in ultimate stress in latewood is mainly due to changes in cell geometry and density but the ultimate stress at the cell wall level increased consistently during the growth period.

The different trends of cell wall stiffness and ultimate stress become even more obvious in the direct comparison with the MFA (Fig. 5). Small changes of cell wall stiffness coincide with small variations in MFA across the growth ring (Fig. 5). Only the first tissue slice showed a slightly higher MFA. However, these findings were contrary to other observations indicating different MFAs in earlywood and latewood (Reiterer et al. 1998; Lichtenegger et al. 1999). Lichtenegger et al. (2003) have shown that MFAs which are measured by cross-field pitting are likely to be overestimated in earlywood.

The trends of stiffness and MFA indicate a close interrelation between both parameters even for very small variations of the cellulose orientation, whereas ultimate stress seems to be decoupled from the cell wall organisation in the cell wall. Therefore, it seems unlikely that changes in MFA and pitting can fully explain the variation of ultimate stress across the growth ring. Considering the trend for the ratio cell wall/cell area (Fig. 2) and the values of ultimate stress and tensile stiffness (cell cross-section) it seems that cell geometry plays a major role. Conceivably, besides changes in the MFA and pitting, tension buckling and structural defects contribute to the reduced ultimate stress. Buckling under tension can be primarily observed in thin-walled fibres, whereas thick-walled fibres resist buckling because the critical buckling stress depends on the response of the fibre to bending stresses in the cell wall (Page and El-Hosseiny 1983). This observation clearly points to a testing artefact for the ultimate stress determination. In the living tree the cells are glued together by the middle lamella. Therefore the individual cells are stabilized by the adjacent cells in the tissue and tension buckling is not likely to occur.

The strategy of the living tree in normal adult wood formation across a growth ring appears to be different from the formation of other tissue types. It was shown in several studies that trees manifest a wide variability of adaptable parameters of cell wall organisation, in particular the cellulose MFA, to adjust mechanical properties of e.g. reaction wood, opposite wood, juvenile wood (e.g. Page and El-Hosseiny 1983; Reiterer et al. 2001; Barnett and Bonham 2004). In our study on the variation of structural and mechanical properties across a growth ring the MFA remained rather constant. Cell wall thickness increased towards the latewood, but it is mainly the cell size that is varied to large extent during the transition from earlywood to latewood. From our findings it seems that Norway spruce optimizes water transport and mechanical stability in normal adult wood on the base of a given "standard of cell wall organisation". The competing functions are addressed during the growth period mainly by the variation of cell size and to a lesser extent by the modulation of the cell wall thickness. Whether the findings presented here are valid for other growth rings, individuals and gymnosperm species remains to be studied.

Conclusions

Variations in the mechanical properties across a growth ring of normal adult wood are mainly related to adaptations at the cell level (cell size) rather than at the cell wall level. This is indicated by small variations of the cellulose microfibril angle which results in a rather constant tensile stiffness of the cell walls. A trend to higher ultimate stress of cell walls across the growth ring is not likely to reflect the mechanical properties in the living tree. It might be explained by tensile buckling of earlywood tracheids in the microtensile testing setup. Our findings suggest that trees manifest a certain "standard of cell wall organisation" in normal adult wood and that mainly cell size and to a lesser extent cell wall thickness is varied to facilitate water transport or mechanical stability during the growth period.

Acknowledgments We wish to thank Paul Zaslansky and John Dunlop for linguistic revision and the "Fonds zur Förderung der wissenschaftlichen Forschung (FWF)" for financial support.

References

Barnett JR, Bonham VA (2004) Cellulose microfibril angle in the cell wall of wood fibres. Biol Rev Camb Philos Soc 79:461–472. doi:10.1017/S1464793103006377

Burgert I, Keckes J, Frühmann K, Fratzl P, Tschegg SE (2002) A comparison of two techniques for wood fiber isolation–evaluation by tensile tests of single fibres with different microfibril angle. Plant Biol 4:9–12. doi:10.1055/s-2002-20430

Burgert I, Frühmann K, Keckes J, Fratzl P, Stanzl-Tschegg SE (2003) Microtensile testing of wood fibers combined with video extensometry for efficient strain detection. Holzforschung 57:661–664. doi:10.1515/HF.2003.099

Burgert I, Frühmann K, Keckes J, Fratzl P, Stanzl-Tschegg S (2004) Structure–function-relationships of four compression wood types—micromechanical properties at the tissue and fibre level. Trees (Berl West) 18:480–485. doi:10.1007/s00468-004-0334-y

Burgert I, Gierlinger N, Zimmermann T (2005a) Properties of chemically and mechanically isolated fibres of spruce (*Picea abies* [L] Karst.). Part 1: structural and chemical characterisation. Holzforschung 59:240–246. doi:10.1515/HF.2005.038

Burgert I, Eder M, Frühmann K, Keckes J, Fratzl P, Stanzl-Tschegg S (2005b) Properties of chemically and mechanically isolated fibres of spruce (*Picea abies* [L] Karst.). Part 3: mechanical characterisation. Holzforschung 59:354–357. doi:10.1515/HF.2005.058

Burgert I, Eder M, Gierlinger N, Fratzl P (2007) Tensile and compressive stresses in tracheids are induced by swelling based on geometrical constraints of the wood cell. Planta 226:981–987. doi:10.1007/s00425-007-0544-9

Cramer SM, Kretschmann D, Lakes R, Schmidt T (2005) Earlywood and latewood elastic properties in loblolly pine. Holzforschung 59:531–538. doi:10.1515/HF.2005.088

Färber J, Lichtenegger HC, Reiterer A, Stanzl-Tschegg S, Fratzl P (2001) Cellulose microfibril angles in a spruce branch and mechanical implications. J Mater Sci 36:5087–8092. doi:10.1023/A:1012465005607

Futó LP (1969) Qualitative und quantitative Ermittlung der Mikrozug-eigenschaften von Holz. Holz Roh- Werkstoff 27:192–201

Groom L, Mott L, Shaler S (2002) Mechanical properties of individual southern pine fibers. Part I. Determination and variability of stress-strain curves with respect to tree height and juvenility. Wood Fiber Sci 34:14–27

Ifju G, Kennedy RW (1962) Some variables affecting microtensile strength of Douglas-Fir. Forest Prod J: 213–217

Jagels R, Visscher GE (2006) A synchronous increase in hydraulic conductive capacity and mechanical support in conifers with relatively uniform xylem structure. Am J Bot 93:179–187. doi:10.3732/ajb.93.2.179

Jernkvist LO, Thuvander F (2001) Experimental determination of stiffness variation across growth rings in *Picea abies*. Holzforschung 55:309–317. doi:10.1515/HF.2001.051

Keckes J, Burgert I, Frühmann K, Müller M, Kölln K, Hamilton M et al (2003) Cell-wall recovery after irreversible deformation of wood. Nat Mater 2:810–814. doi:10.1038/nmat1019

Lichtenegger HC, Reiterer A, Tschegg S, Fratzl P (1998) Determination of spiral angles of elementary fibrils in the wood cell wall: comparison of small-angle X-ray scatering and wide-angle X-ray diffraction. In: Butterfield BG (ed) Microfibril angle in wood, Proceedings of the IAWA/IUFRO international workshop on the significance of microfibril angle to wood quality. Westport, New Zealand, pp 140–156

Lichtenegger HC, Reiterer A, Stanzl-Tschegg SE, Fratzl P (1999) Variation of cellulose microfibril angles in softwoods and hardwoods—a possible strategy of mechanical optimization. J Struct Biol 129:257–269. doi:10.1006/jsbi.1999.4194

Lichtenegger HC, Müller M, Wimmer R, Fratzl P (2003) Microfibril angles inside and outside crossfields of Norway spruce tracheids. Holzforschung 57:13–20. doi:10.1515/HF.2003.003

Mott L, Groom L, Shaler S (2002) Mechanical properties of individual Southern pine fibers. Part II. Comparison of earlywood and latewood fibers with respect to tree height and juvenility. Wood Fiber Sci 34:221–237

Niklas KJ (1992) Plant biomechanics: an engineering approach to plant form and function. University of Chicago Press, Chicago, USA

Page DH, El-Hosseiny F, Winkler K, Lancaster APS (1977) Elastic modulus of single wood pulp fibers. Tappi 60:114–117

Page DH, El-Hosseiny F (1983) The mechanical properties of single wood pulp fibres. Part VI. Fibril angle and the shape of the stress-strain curve. J Pulp Pap Sci 9:1–2

Reiterer A, Jakob HF, Stanzl-Tschegg SE, Fratzl P (1998) Spiral angle of elementary cellulose fibrils in cell walls of *Picea abies* determined by small-angle X-ray scattering. Wood Sci Technol 32:335–345. doi:10.1007/BF00702790

Reiterer A, Lichtenegger HC, Fratzl P, Stanzl-Tschegg SE (2001) Deformation and energy absorption of wood cell walls with different nanostructure under tensile loading. J Mater Sci 36:4681–4686. doi:10.1023/A:1017906400924

Schniewind AP (1966) Über Unterschiede in der Zugfestigkeit von Früh- und Spätholztracheiden. Holz Roh- Werkstoff 24:502–510

Yamamoto H (1999) A model of the anisotropic swelling and shrinking process of wood. Part1. Generalization of Barber's wood fiber model. Wood Sci Technol 33:311–325. doi:10.1007/s002260050118

Yamamoto H, Sassus F, Ninomiya M, Gril J (2001) A model of anisotropic swelling and shrinking process of wood. Wood Sci Technol 35:167–181. doi:10.1007/s002260000074